

Facile electrochemical synthesis of triangle-shaped graphene nanoflakes and graphene quantum dots via surfactant-assisted and defect-induced mechanism

Wan Hazman Danial^{1*}, Noriliya Aina Norhisham¹, Ahmad Fakhurrazi Ahmad Noorden², and Zaiton Abdul Majid³

¹Department of Chemistry, Kulliyah of Science, International Islamic University Malaysia, 25200 Kuantan, Pahang, Malaysia

²Advanced Optoelectronics Research Group (CAPTOR), Department of Physics, Kulliyah of Science, International Islamic University Malaysia, 25200 Kuantan, Pahang, Malaysia

³Department of Chemistry, Faculty of Science, University Teknologi Malaysia, 81310 UTM Johor Bahru, Johor, Malaysia

*Corresponding author. E-mail: whazman@iium.edu.my

Received: Dec. 12, 2020; Accepted: May 10, 2021

A facile and non-hazardous route for synthesis of triangle-shaped graphene nanoflakes and graphene quantum dots (GQDs) suspension *via* electrochemical exfoliation has been reported. In this work, a simple electrochemical technique was employed using pristine and heated graphite electrodes under the influence of anionic surfactant, sodium dodecylbenzene sulfonate (SDBS). The synthesized graphene nanoflakes and GQDs suspension were characterized using UV-visible spectroscopy, transmission electron microscope (TEM) and Raman Spectroscopy. The UV absorption spectra showed a bathochromic shift from the typical $\pi \rightarrow \pi^*$ transition peak which due to the introduction of oxygen groups and/or functionalization of SDBS into the graphitic layers. Morphological analyses using TEM revealed the usage of heated graphite electrodes (600 °C at 5 min) produced a triangle-shaped graphene nanoflakes with an average size of ~ 34 nm while the average size of the graphene nanoflakes obtained using the pristine graphite is ~ 47 nm. A possible mechanism for the exfoliation of such morphology has been proposed. The graphene nanoflakes which have size less than 10 nm from both samples can be attributed to the presence of the GQDs. Raman analysis revealed I_D/I_G ratio of 0.223 and 0.203 for graphene nanoflakes electrochemically exfoliated from pristine and heated graphite respectively, which signifies a better quality and crystallinity and has low defects within the conjugated graphene backbone. The utilization of this electrochemical approach might expectantly pave the way towards the production of graphene nanoflakes with controlled morphology and low structural defects, which can be an efficient top-down process yet feasible for mass production.

Keywords: Electrochemical, exfoliation, graphene nanoflakes, graphene quantum dots, triangle-shaped

© The Author(s). This is an open access article distributed under the terms of the [Creative Commons Attribution License \(CC BY 4.0\)](https://creativecommons.org/licenses/by/4.0/), which permits unrestricted use, distribution, and reproduction in any medium, provided the original author and source are cited.

[http://dx.doi.org/10.6180/jase.202206_25\(3\).0016](http://dx.doi.org/10.6180/jase.202206_25(3).0016)

1. Introduction

Graphene, a 2D crystalline material with sp^2 hybridized carbon structure have been emerging back-to-back in creating wide range of novelties, which drives the global demand to develop graphene and graphene-based materials

using various approaches. Albeit ideally consist of pure sp^2 carbon bonds, graphene realistically varies in size, thickness and surface defects which very much dependent on the preparation technique [1]. Number of techniques have been reported to produce graphene from a range of precursors, chemicals and conditions parameters. However,

several weakness and drawbacks in the methods that thus far employed need to be addressed. For instance, the scotch tape method [2] is neither high throughput nor high yield. The chemical exfoliation methods [3–5] required the usage of strong acidic and oxidising chemicals which can be hazardous and suffer with complicated washing procedures. The chemical vapor deposition [6] required crucial control of the conditions after nucleating a sheet while the organic synthesis [7] required complicated reaction setup and produce side reactions.

By contrast, electrochemical exfoliation method is considered to be facile and promising technique to curb these matters [8, 9]. The electrochemical route have occasionally fabricated several forms of graphene materials with different properties and functionalities in different types of electrolytes such as organic solvents [10, 11], ionic liquids [12, 13] and mineral acids [14, 15]. Among various options, an anionic surfactant called sodium dodecyl benzene sulfonate (SDBS) has been used in the electrochemical synthesis of graphene. SDBS is one of the amphiphilic surfactants that provides a high degree of exfoliation and dispersion where the hydrophobic tail adsorbs onto graphite for exfoliation while the hydrophilic heads facilitate the dispersion through electrostatic repulsion [16]. The electrochemical technique is one of the top-down approach which involve the exfoliation of bulk graphite, broken down into smaller particles forming graphene flakes. Nano-size graphene flakes is considered as graphene nanoflakes [17] or sometimes known as graphene nanoplatelets, often appeared with arbitrary shape and lateral dimension. Much smaller particle derived from the graphene flakes produce a quasi-zero-dimensional nanostructures, known as graphene quantum dots (GQDs) [18].

In this work, we report a facile, simple and environmentally friendly method to synthesis graphene nanoflakes and GQDs from pristine and defect-induced graphite rods with the assistance of sodium dodecylbenzene sulfonate (SDBS) as the electrolyte. The defect-induced graphite rods were obtained by heating at high temperature with the purpose of providing more surface defects and available sites for intercalation, thus facilitates the electrochemical exfoliation of smaller graphene particles or nanoflakes [19]. To the best of our knowledge, the production of graphene nanoflakes using the combination of the said surfactant and defect-induced electrode has not yet been reported. Material characterization was carried out using UV-visible spectroscopy, transmission electron microscope (TEM), high-resolution transmission electron microscope (HRTEM) and Raman spectroscopy to investigate the effect of using pristine and heated graphite electrodes via the influence of anionic sur-

factant towards the morphology and size distribution of the graphene nanoflakes. The electrochemical exfoliation method has been recognised as one of the efficient top-down techniques in producing graphene and GQDs [9]. Since the technique offer the production of stable colloidal graphene nanoflakes, it significantly overcome any non-dispersibility issue and allow a direct assembly of the suspension for example in composite preparation for polymer [20] and engineering application [21]. Therefore, the prepared graphene nanoflakes and GQDs with the assistance of anionic surfactant (SDBS) may pave the way towards various technological applications of the nanomaterial.

2. Methodology

2.1. Materials

All the chemicals in this research were used without any pre-treatment. Sodium dodecyl benzene sulphonate (SDBS) was supplied by Sigma-Aldrich, USA. The graphite rods (99.99%) used were purchased from Niahode, China while the DC power supply (Wanptek) was purchased from Hitechrons Sdn. Bhd., Johor, Malaysia. Graphite powder was purchased from Sigma-Aldrich, USA and was used as a reference material.

2.2. Preparation of electrolyte and electrode

The study utilized aqueous anionic surfactant, SDBS as the electrolyte. 0.3424 g of SDBS was weighed and dissolved in 500 mL of deionized water to obtain a concentration of 0.002 M. Two sets of electrolytes of the same concentration were prepared and two pair of graphite rods were weighed and the length and diameter were measured. A pair of pristine graphite rods were used without any treatment while another pair of graphite rod were furnace at 600 °C for 5 min to introduce a surface defect. The defect-induced graphite electrodes were allowed to cool to room temperature and again the weight and dimensions were recorded. Prior to the experiment, all graphite rods including the pristine graphite (without furnace) were washed with deionized water to remove any large particles and dried.

2.3. Electrochemical exfoliation

A simple two-electrode cell system was employed for the electrochemical exfoliation of graphene nanoflakes and triangle-shaped graphene nanoflakes as presented in Fig. 1 and the entire process was operated at room temperature. The pristine graphite rods (10.1 cm in length and diameter of 1 cm) were set as both anode and cathode, with working distance of 3 cm dipped in 0.002 M of SDBS electrolyte. The pristine graphite rods were electrochemically exfoliated at 7

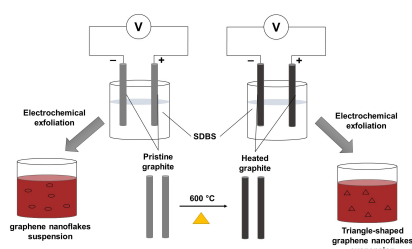


Fig. 1. Schematic illustration of electrochemical synthesis of triangle-shaped graphene nanoflakes.

V for a total of 15 h adapting similar electrochemical mechanism reported by Danial et al. [8]. During the reaction, the electrolyte gradually changed from colourless to brown suspension. The suspension was then sonicated for 30 min, shaken vigorously and further dialyzed using a 3500 Da dialysis bag for more than a week against deionized water to remove any ions. The procedure was repeated using defect-induced graphite rods (furnaced at 600 °C for 5 min, 10.1 cm in length and diameter of 1 cm) but with an applied voltage of 17 V, to achieve the same current (A) value with the pristine graphite electrodes.

2.4. Characterization

The pristine and furnaced graphite electrodes were analyzed using FTIR (Perkin Elmer). A pure graphite powder (Sigma Aldrich) was analyzed as a reference material. The FTIR analysis was carried out using attenuated total reflection (ATR) technique and the infrared absorption spectra were obtained in the range of 4000-600 cm^{-1} . UV-vis spectra were obtained using double beam UV-Vis spectrometer (Perkin Elmer) to analyze the suspension produced with 0.002 M of SDBS as a blank. Imaging analysis using Zeiss Libra 120 Transmission electron microscope (TEM) was performed to investigate the morphology and size distribution of graphene and GQDs suspension produced. The solution was drop-casted on a carbon grid double film 200 mesh followed by an oven drying for 15-30 min at 37 °C. High resolution images were recorded using a field-emission electron microscope (JEOL JEM-ARM200F) operated at an accelerating voltage of 200 kV. Raman spectra were recorded using Horiba LabRAM HR Evolution spectrometer with Argon gas at 514 nm laser excitation source within the range 800 – 3000 cm^{-1} .

3. Results and Discussion

3.1. Electrochemical exfoliation of graphene nanoflakes and GQDs

In this study, a colloidal brown suspension was obtained to indicate the electrochemical exfoliation of the graphite

electrode was successful with the assistance of the anionic surfactant, SDBS which was used as the electrolyte for providing both sulphate source and electrolysis environment. The dissociation of SDBS into solution produces ions with a much larger size as compared to the SO_4^{2-} ions produced from H_2SO_4 or NaSO_4 [22], thusly play a significant role for the electrochemical expansion of the graphite. The presence of benzene ring allows the anions to interact with the graphitic layers via π - π interaction thus making the electrochemical exfoliation process much feasible [22]. During the electrochemical process, the proposed mechanism involved is as follows: 1) intercalation and accumulation ions into the graphitic layers via electrostatic interaction; 2) expansion of interlayer spacing between adjacent graphene to be greater than 3.35Å [23]; 3) weakening of van der Waals forces between the adjacent layers; 4) exfoliation of graphitic layers via subsequent electrostatic repulsion. The overall mechanism of electrochemical exfoliation occurred for the production of graphene nanoflakes and GQDs in this study is presented in Fig. 2. It is worth mentioning that the usage of defect-induced graphite electrode will affects the electrochemical exfoliation mechanism. As illustrated in the figure, the surface of the furnaced graphite will consist of defect hole, which in turn determine the morphology or size of the exfoliated graphene nanoflakes. In this study, the production of triangle-shaped graphene nanoflakes is proposed through the mechanism highlighted.

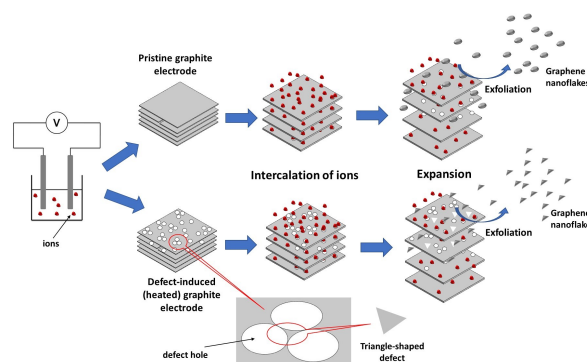
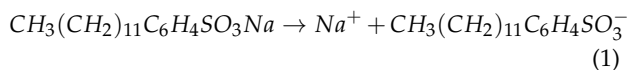


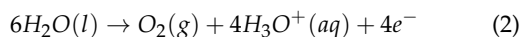
Fig. 2. The proposed mechanism for the electrochemical exfoliation of triangle-shaped graphene nanoflakes.

In this experiment, as the SDBS dissolved in water, portions of the SDBS molecules dissociates into Na^+ and negatively charged complex ions, $\text{CH}_3(\text{CH}_2)_{11}\text{C}_6\text{H}_4\text{SO}_3^-$ (Eq. 1). When potential voltage is applied, redox reaction takes place where the positive terminal anode attracts anions and causes oxidation to occur (Eq. 2) while the negative terminal cathode attracts cations that results to reduction reaction (Eq. 3). The hydroxyl ions suspended in the solution will compete with the $\text{CH}_3(\text{CH}_2)_{11}\text{C}_6\text{H}_4\text{SO}_3^-$

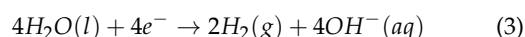
ion to be adsorbed into the electropositive position of the graphitic surface.



Anode:



Cathode:



In addition, the voltage applied plays an important role on the type of graphene nanoflakes and GQDs being produced in terms of its oxidation degree, defect density, size and morphology of the product. If the applied potential is too low, the graphene sheet will not be separated and if it is too high, separation of several stacked multilayer sheets from the electrode may take place [22]. In dilute or moderately concentrated salt solutions, water splitting commonly occur at a minimum potential difference of 1.23 V and will eventually cause oxygen gas being produced at the anode. The potential voltage applied in this study is above the said potential which allow the formation of the gas bubbles.

3.1.1. Pristine graphite rods.

The pristine graphite rods (as anode and cathode) were electrochemically exfoliated at potential voltage of 7 V for a total period of 15 h / 900 min. As can be seen in Fig. 3, the colour of the electrolyte changes significantly from colourless to brownish as the time of exfoliation increases. Bubbles were visually observed at the working electrode. This proves that the exfoliation mechanism was involved throughout the entire reaction.

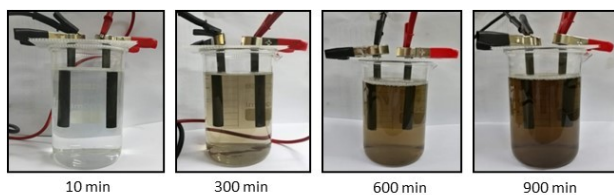


Fig. 3. Electrochemical synthesis of graphene nanoflakes from pristine graphite rods at 10, 300, 600 and 900 min.

3.1.2. Defect-induced graphite rods.

At 7 V potential voltage, there is no significant electrochemical exfoliation occurred using the defect induced graphite rods (as anode and cathode) and the electrolyte remain

colorless without any change in colour to indicate any exfoliation. It is expected the electrical conductivity of the graphite rods was affected due to the defect-induced surface and graphitic backbone disruption when introduced with heat at 600 °C for 5 min. The heating treatment may cause a number microcracks and pores on the graphite structure, which hindered the conductivity and resulted in the increase of electrical resistivity [24]. However, when the potential voltage was increased to 17 V (reached similar current value as compared to when using the pristine graphite electrodes), the colour of electrolyte then changes gradually from colourless to pale brown (See Fig. 4) but appeared not as concentrated as the suspension produced using the pristine graphite electrodes. Obvious bubbles formation was also observed at both of the electrodes. This shows that similar mechanism took place during the electrochemically exfoliation process but required higher potential voltage to achieve the same current value.

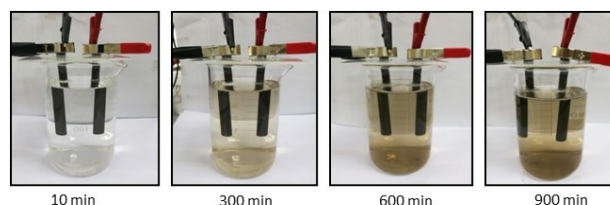


Fig. 4. Electrochemical synthesis of graphene nanoflakes from heated graphite rods at 10, 300, 600 and 900 min with an applied voltage of 17 V.

3.2. FTIR analysis of electrode

FTIR analysis was preliminary performed to characterize the carbon structures of the graphite electrodes based on the vibrational frequencies. In general, few absorption signals were observed for all of the graphite samples due to the difference in the state of charges between carbon atoms [25]. A very small induced electric dipole due to the weak differences lead to the clean spectrum and showed no significant peaks pertinent to any functional groups for all samples. As shown in Fig. 5, the pristine graphite rods provide identical FTIR spectrum as compared to the pure graphite (Sigma Aldrich) as a reference. and heated at 600 °C graphite rods showed similar peaks to the pure graphite (Sigma-Aldrich) as a reference. This indicates that the graphite rods purchased were authentic to be used in the electrochemical process. In addition, the heated graphited rods (600 °C) also showed similar spectrum with the pristine and pure graphite.

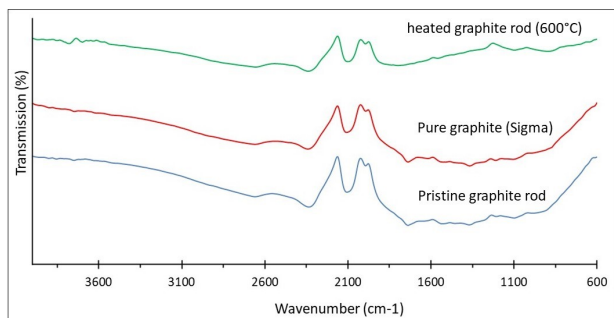


Fig. 5. FTIR spectra of the pristine graphite rod, pure graphite (Sigma-Adrich) and heated graphite rod.

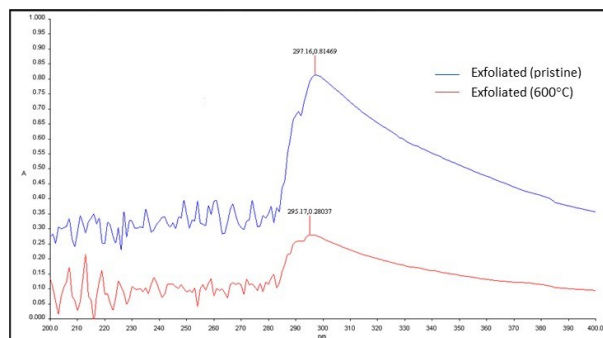


Fig. 6. UV-Vis absorption spectra of exfoliated sample suspension from pristine and heated graphite electrodes.

3.3. UV-vis spectroscopy

The UV-Vis absorption spectra for both exfoliated samples (suspensions) produced using pristine and heated graphite electrodes are shown in Fig. 6. The maximum absorbance around 295 – 297 nm were obtained for both suspensions. As compared to the typical $\pi \rightarrow \pi^*$ transition of the C=C bonds of graphene at 268 nm [26, 27], both samples, however, showed $\sim 27 - 29$ nm bathochromic shift of the maximum absorbance. This might be due to the existence of oxygenated compound presence in the colloidal suspensions which corresponds to $n \rightarrow \pi^*$ transition of C=O bond [28]. The $n \rightarrow \pi^*$ transition of C=O might also come from the sulphate source which is in agreement with the work of Peng et al. [29]. Besides, the absorption spectra provide evidence on the graphite exfoliation as well as functionalization of SDBS into the graphitic structure. The higher absorbance intensity for the sample obtained using the pristine graphite indicates more exfoliated product was produced, as observed in Fig. 3, which showed darker suspension as compared to sample obtained using heated graphite rods. The presence of some noisy peaks below 280 nm^{-1} for both graphene nanoflakes suspensions might be due to the slight deviation of the solvent (electrolyte) from the original blank solution (0.002M SDBS), whereby the ions had participated in the electrochemical interaction for the graphene production.

3.4. Transmission electron microscope (TEM)

Fig. 7 shows the TEM images of the colloidal suspension obtained using the pristine graphite electrodes. Fig. 7a and 7b shows the presence of small size graphene particles produced, which resulted from the electrochemical exfoliation process. This small size graphene particles can be considered as graphene nanoflakes and the inset image depict the size distribution of the nanoflakes which ranges between 10 to 130 nm with an average size of ~ 47 nm. Based on the size distribution, around 80% of the graphene nanoflakes has

size in the range 10 – 60 nm. At higher magnification image (Fig. 7c), less than 10 nm size can also be found which might correspond to the presence of graphene quantum dots (GQDs), albeit enclosed or agglomerated within the graphene flakes structure. The corresponding histogram in the inset image (Fig. 7c) shows the size distribution of the GQDs with the average size of 5.7 nm. Fig. 7d shows the high-resolution image of the graphene nanoflakes in which the hexagonal lattice spacing value of 0.21 was obtained, which attributed to the lattice constant of graphene or GQDs [19].

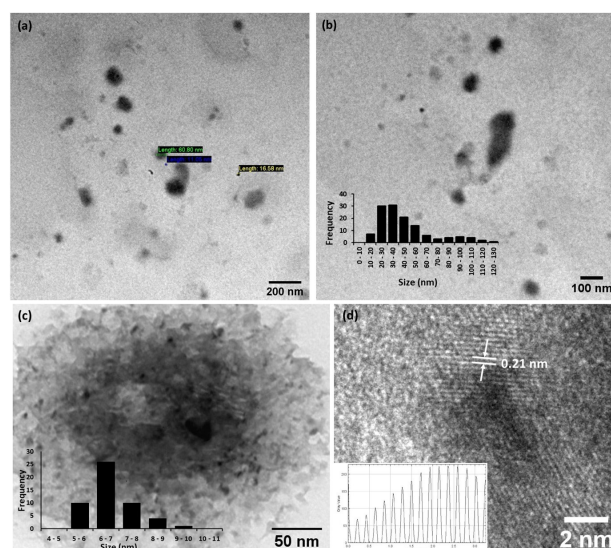


Fig. 7. TEM images of graphene nanoflakes and GQDs from pristine graphite. The inset is the particle size distribution.

Fig. 8 shows TEM images of the colloidal suspension obtained using the heated graphite electrodes. The TEM images indicate the production of triangle-shaped graphene nanoflakes was achieved when the heated (defect-induced) graphite electrode was used for the electrochemical exfo-

liation process. The triangular shape was prominent and clearly observed in the TEM images (Fig. 8a and 8b) and the corresponding histogram shown in the inset revealed that graphene nanoflakes obtained has an average size of ~ 34 nm with more than $\sim 80\%$ ranged between 20 and 60 nm. Some of the graphene nanoflakes obtained of less than 10 nm can be ascribed to the presence of GQDs in the suspension. Fig. 8c is high-resolution TEM image which depict the presence of heart-shaped graphene nanoflake can also be found attributed from the triangle-shaped nanoflakes. A thin and relatively transparent image of the graphene can also be observed (Fig. 8c) which corresponds to the typical graphene image. Fig. 8d shows the high-resolution image of the graphene nanoflakes in which lattice spacing value of 0.24 was obtained, which ascribed to the hexagonal (1120) lattice fringes of the graphene [30].

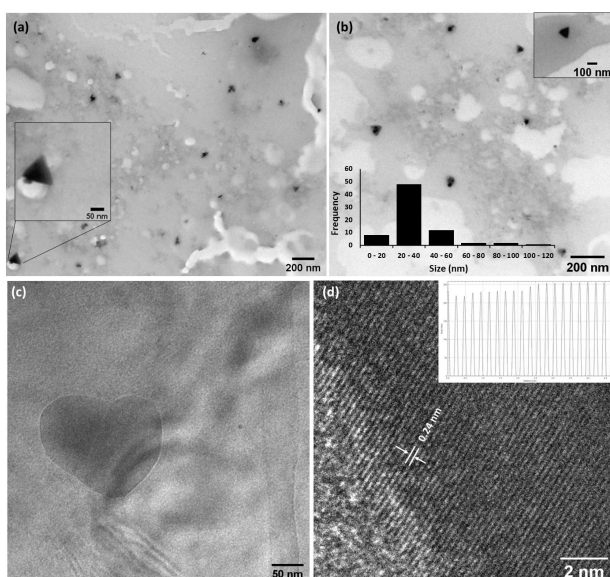


Fig. 8. TEM images of graphene nanoflakes and GQDs from heated graphite. The inset is the particle size distribution.

3.5. Raman spectroscopy

Raman Spectroscopy analysis was carried out to characterize the molecular backbones and to investigate the graphitic configuration effects of the exfoliated graphene nanoflakes obtained from the colloidal suspensions. The Raman spectrum of graphene commonly features three characteristic peaks which represents D, G and 2D bands. The D band reflects the degree of defects in the graphene structure which comes from the breathing mode of sp^3 hybridized carbon atoms, while the G band corresponds to the in-plane vibrational mode of sp^2 carbon atoms [31, 32]. The 2D band (also known as an overtone of D band) is due to two phonons

of double resonance transitions with an opposite momentum and the shift and shape corresponds to the number of graphene layers [33]. As for the intensity ratio of the D band to G band (I_D/I_G), it has been generally useful to evaluate the degree of graphene defects. Fig. 9 shows the Raman spectra for graphene nanoflakes samples produced from both pristine and heated graphite electrodes, which observed to have D band at around 1347.42 cm^{-1} and G band at around 1574.04 cm^{-1} with I_D/I_G ratio less than 1. The graphene nanoflakes sample obtained via electrochemical exfoliation of the pristine graphite give I_D/I_G value of 0.223 while graphene nanoflakes produced from heated graphite depict I_D/I_G value of 0.203. The low ratio indicates that the graphene nanoflakes have relatively small number of defects, higher extent of crystallinity and better integrity when compared to the graphene ($I_D/I_G = 1.24\text{ cm}^{-1}$) exfoliated using Na_2SO_4 in the work of Zhao et al. [34]. It is also expected that the lower ratio is associated with less structural defects on the surface of the graphene nanoflakes in both samples [19]. This also suggest that although the graphite was introduced with surface defects (as a whole), the structural backbone quality was maintained within the graphene nanoflakes after the exfoliation process. Moreover, the weak and narrow D band observed is quite similar to the D band of GQDs observed in the Raman spectrum of Huang et al. [32], which then suggests that the functionalization of SDBS does not destroy the conjugated backbone of graphene sp^2 carbon. The low intensity of 2D band appeared at around 2709.22 cm^{-1} for both samples signifies the presence of few layers of graphene which might be due to samples being re-aggregated or folded during their preparation [14].

4. Conclusions

In conclusion, different types of graphite electrode (pristine or heated) operating at similar electric current affect the morphology and size distribution of the graphene nanoflakes and GQDs obtained. Stable colloidal of graphene nanoflakes and GQDs in two aqueous suspensions were successfully synthesised from the pristine graphite and defect-induced graphite rod via top-down electrochemical exfoliation technique with the assistance of an anionic surfactant, SDBS. The exfoliation of graphene nanoflakes were observed through the colour change of the electrolyte used from colourless to brownish. The FTIR spectra confirmed the authenticity of the graphite rods used by having similar peaks with the pure graphite powder (Sigma-Aldrich) as a reference, and the heated graphite rods produced similar FTIR spectrum which indicates the graphitic structure integrity was maintained albeit some

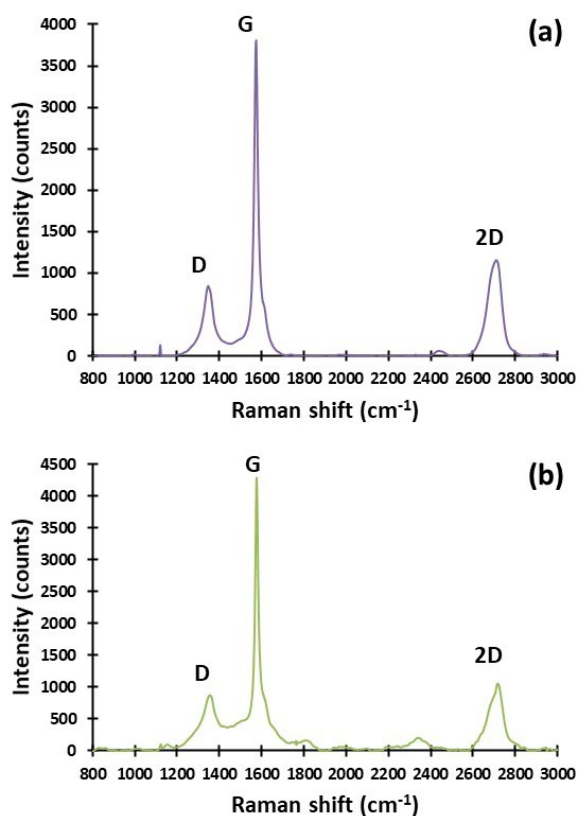


Fig. 9. Raman spectrum for graphene nanoflakes produced from (a) pristine graphite and (b) heated graphite.

surface defects might be induced. The UV absorption spectra depicted a red shift from the typical $\pi \rightarrow \pi^*$ transition of the C=C bonds of graphene at 268 nm which might be due to oxidation and/or functionalization of SDBS into the graphene nanoflakes or GQDs. The presence of the graphene nanoflakes produced from the electrochemical exfoliation of pristine graphite can be observed under TEM imaging analysis and 80% of the nanoflakes exhibited size ranging from 10 to 60 nm. The usage of heated or defect-induced graphite rods produced a distribution of triangle-shaped graphene nanoflakes with an average size of ~ 34 nm based on the suggested exfoliation mechanism. The presence of less than 10 nm size of the graphene nanoflakes from both samples can be ascribed to the presence of the GQDs. The Raman spectra substantiated the presence of retained graphene backbone with peak intensity ratio of I_D/I_G of 0.223 and 0.203 for graphene nanoflakes exfoliated from pristine and heated graphite electrode, respectively, which indicates that high quality graphene with relatively small content of defects were successfully prepared. Owing to its colloidal stability and dispersibility, the graphene nanoflakes is potentially useful for nanocomposites appli-

cation with a wide range of targeted matrix through direct assembly and solution mixing. The facile, simple and environmentally friendly method could contribute to the future works in the synthesis of graphene nanoflakes and GQDs, and might have a significant potential to be explored for various applications.

Acknowledgements

This work was supported by the Fundamental Research Grant Scheme (Reference code: FRGS/1/2018/STG01/UIAM/03/2) (Project ID: FRGS19-015-0623), Ministry of Higher Education (MOHE), Malaysia and Department of Chemistry, Kulliyah of Science, International Islamic University Malaysia.

References

- [1] Kong W., Kum H., Bae S. H., Shim J., Kim H., Kong L., Meng Y., Wang K., Kim, C. and Kim J., (2019) "Path towards graphene commercialization lab to market" **Nature Nanotechnology** 14(10): 927–938. DOI: <https://doi.org/10.1038/s41565-019-0555-2>.
- [2] K. S. Novoselov, A. K. Geim, S. V. Morozov, D. Jiang, Y. Zhang, S. V. Dubonos, I. V. Grigorieva, and A. A. Firsov, (2004) "Electric field in atomically thin carbon films" **Science** 306(5696): 666–669. DOI: [10.1126/science.1102896](https://doi.org/10.1126/science.1102896).
- [3] S. Wei, R. Zhang, Y. Liu, H. Ding, and Y. L. Zhang, (2016) "Graphene quantum dots prepared from chemical exfoliation of multiwall carbon nanotubes: An efficient photocatalyst promoter" **Catalysis Communications** 74: 104–109. DOI: [10.1016/j.catcom.2015.11.010](https://doi.org/10.1016/j.catcom.2015.11.010).
- [4] E. Kusriani, F. Oktavianto, A. Usman, D. P. Mawarni, and M. I. Alhamid, (2020) "Synthesis, characterization, and performance of graphene oxide and phosphorylated graphene oxide as additive in water-based drilling fluids" **Applied Surface Science** 506: 145005. DOI: [10.1016/j.apsusc.2019.145005](https://doi.org/10.1016/j.apsusc.2019.145005).
- [5] E. Kusriani, A. Suhrowati, A. Usman, M. Khalil, and V. Degirmenci, (2019) "Synthesis and characterization of graphite oxide, graphene oxide, and reduced graphene oxide from graphite waste using modified hummers' method and zinc as reducing agent" **International Journal of Technology** 10(6): 1093–1104. DOI: [10.14716/ijtech.v10i6.3639](https://doi.org/10.14716/ijtech.v10i6.3639).
- [6] F. Qing, Y. Hou, R. Stehle, and X. Li, (2019) "Chemical vapor deposition synthesis of graphene films" **APL Materials** 7(2): 020903. DOI: [10.1063/1.5078551](https://doi.org/10.1063/1.5078551).

- [7] S. H. Lee, D. Y. Kim, J. Lee, S. B. Lee, H. Han, Y. Y. Kim, S. C. Mun, S. H. Im, T. H. Kim, and O. O. Park, (2019) "Synthesis of Single-Crystalline Hexagonal Graphene Quantum Dots from Solution Chemistry" **Nano Letters** 19(8): 5437–5442. DOI: [10.1021/acs.nanolett.9b01940](https://doi.org/10.1021/acs.nanolett.9b01940).
- [8] W. H. Danial, A. Chutia, Z. A. Majid, R. Sahnoun, and M. Aziz. "Electrochemical synthesis and characterization of stable colloidal suspension of graphene using two-electrode cell system". In: *AIP Conference Proceedings*. 1669. 2015, 020020. DOI: [10.1063/1.4919158](https://doi.org/10.1063/1.4919158).
- [9] W. H. Danial, N. A. Norhisham, A. F. Ahmad Noorden, Z. Abdul Majid, K. Matsumura, and A. Iqbal. *A short review on electrochemical exfoliation of graphene and graphene quantum dots*. 2021. DOI: [10.1007/s42823-020-00212-3](https://doi.org/10.1007/s42823-020-00212-3).
- [10] Y. L. Zhong and T. M. Swager, (2012) "Enhanced electrochemical expansion of graphite for in situ electrochemical functionalization" **Journal of the American Chemical Society** 134(43): 17896–17899. DOI: [10.1021/ja309023f](https://doi.org/10.1021/ja309023f).
- [11] X. Wang and L. Zhang, (2019) "Green and facile production of high-quality graphene from graphite by the combination of hydroxyl radicals and electrical exfoliation in different electrolyte systems" **RSC Advances** 9(7): 3693–3703. DOI: [10.1039/c8ra09752f](https://doi.org/10.1039/c8ra09752f).
- [12] A. Ananthanarayanan, X. Wang, P. Routh, B. Sana, S. Lim, D. H. Kim, K. H. Lim, J. Li, and P. Chen, (2014) "Facile synthesis of graphene quantum dots from 3D graphene and their application for Fe³⁺ sensing" **Advanced Functional Materials** 24(20): 3021–3026. DOI: [10.1002/adfm.201303441](https://doi.org/10.1002/adfm.201303441).
- [13] Y. Yan, H. Li, Q. Wang, H. Mao, and W. Kun, (2017) "Controllable ionic liquid-assisted electrochemical exfoliation of carbon fibers for the green and large-scale preparation of functionalized graphene quantum dots endowed with multicolor emission and size tunability" **Journal of Materials Chemistry C** 5(24): 6092–6100. DOI: [10.1039/c7tc01342f](https://doi.org/10.1039/c7tc01342f).
- [14] S. Yang, S. Brüller, Z. S. Wu, Z. Liu, K. Parvez, R. Dong, F. Richard, P. Samorì, X. Feng, and K. Müllen, (2015) "Organic Radical-Assisted Electrochemical Exfoliation for the Scalable Production of High-Quality Graphene" **Journal of the American Chemical Society** 137(43): 13927–13932. DOI: [10.1021/jacs.5b09000](https://doi.org/10.1021/jacs.5b09000).
- [15] Y. Z. Htwe, W. S. Chow, Y. Suda, A. A. Thant, and M. Mariatti, (2019) "Effect of electrolytes and sonication times on the formation of graphene using an electrochemical exfoliation process" **Applied Surface Science** 469: 951–961. DOI: [10.1016/j.apsusc.2018.11.029](https://doi.org/10.1016/j.apsusc.2018.11.029).
- [16] Q. Zhou, G. Xia, M. Du, Y. Lu, and H. Xu, (2019) "Scotch-tape-like exfoliation effect of graphene quantum dots for efficient preparation of graphene nanosheets in water" **Applied Surface Science** 483: 52–59. DOI: [10.1016/j.apsusc.2019.03.290](https://doi.org/10.1016/j.apsusc.2019.03.290).
- [17] S. Mutyala and J. Mathiyarasu, (2015) "Preparation of graphene nanoflakes and its application for detection of hydrazine" **Sensors and Actuators, B: Chemical** 210: 692–699. DOI: [10.1016/j.snb.2015.01.033](https://doi.org/10.1016/j.snb.2015.01.033).
- [18] C. Mansilla Wettstein, F. P. Bonafé, M. B. Oviedo, and C. G. Sánchez, (2016) "Optical properties of graphene nanoflakes: Shape matters" **Journal of Chemical Physics** 144(22): 224305. DOI: [10.1063/1.4953172](https://doi.org/10.1063/1.4953172). arXiv: [1512.00489](https://arxiv.org/abs/1512.00489).
- [19] S. Ahirwar, S. Mallick, and D. Bahadur, (2017) "Electrochemical Method to Prepare Graphene Quantum Dots and Graphene Oxide Quantum Dots" **ACS Omega** 2(11): 8343–8353. DOI: [10.1021/acsomega.7b01539](https://doi.org/10.1021/acsomega.7b01539).
- [20] M. J. Nine, T. T. Tung, and D. Losic. "Self-Assembly of Graphene Derivatives: Methods, Structures, and Applications". In: *Comprehensive Supramolecular Chemistry II*. 9. Elsevier, 2017, 47–74. DOI: [10.1016/B978-0-12-409547-2.12634-4](https://doi.org/10.1016/B978-0-12-409547-2.12634-4).
- [21] Z. Zhao, P. Bai, W. Du, B. Liu, D. Pan, R. Das, C. Liu, and Z. Guo. *An overview of graphene and its derivatives reinforced metal matrix composites: Preparation, properties and applications*. 2020. DOI: [10.1016/j.carbon.2020.08.040](https://doi.org/10.1016/j.carbon.2020.08.040).
- [22] S. K. Tiwari, A. Huczko, R. Oraon, A. De Adhikari, and G. C. Nayak, (2017) "Facile electrochemical synthesis of few layered graphene from discharged battery electrode and its application for energy storage" **Arabian Journal of Chemistry** 10(4): 556–565. DOI: [10.1016/j.arabjc.2015.08.016](https://doi.org/10.1016/j.arabjc.2015.08.016).
- [23] I. Razado-Colambo, J. Avila, D. Vignaud, S. Godey, X. Wallart, D. P. Woodruff, and M. C. Asensio, (2018) "Structural determination of bilayer graphene on SiC(0001) using synchrotron radiation photoelectron diffraction" **Scientific Reports** 8(1): 10190. DOI: [10.1038/s41598-018-28402-0](https://doi.org/10.1038/s41598-018-28402-0).

- [24] M. Li and R. Luo. "Effect of heating rate on the properties of a graphite/phenolic-based composite". In: *Proceedings of the 5th International Conference on Information Engineering for Mechanics and Materials*. 21. Paris: Atlantis Press, 2015. DOI: [10.2991/icimm-15.2015.104](https://doi.org/10.2991/icimm-15.2015.104).
- [25] S. Ruiz, J. A. Tamayo, J. D. Ospina, D. P. N. Porras, M. E. V. Zapata, J. H. M. Hernandez, C. H. Valencia, F. Zuluaga, and C. D. G. Tovar, (2019) "Antimicrobial films based on nanocomposites of chitosan/poly(Vinyl alcohol)/graphene oxide for biomedical applications" **Biomolecules** 9(3): 109. DOI: [10.3390/biom9030109](https://doi.org/10.3390/biom9030109).
- [26] G. A. Ali, M. R. Thalji, W. C. Soh, H. Algarni, and K. F. Chong, (2020) "One-step electrochemical synthesis of MoS₂/graphene composite for supercapacitor application" **Journal of Solid State Electrochemistry** 24(1): 25–34. DOI: [10.1007/s10008-019-04449-5](https://doi.org/10.1007/s10008-019-04449-5).
- [27] B. Nazari, Z. Ranjbar, R. R. Hashjin, A. Rezvani Moghaddam, G. Momen, and B. Ranjbar, (2019) "Dispersing graphene in aqueous media: Investigating the effect of different surfactants" **Colloids and Surfaces A: Physicochemical and Engineering Aspects** 582: 123870. DOI: [10.1016/j.colsurfa.2019.123870](https://doi.org/10.1016/j.colsurfa.2019.123870).
- [28] S. Li, Y. Chen, X. He, X. Mao, Y. Zhou, J. Xu, and Y. Yang, (2019) "Modifying Reduced Graphene Oxide by Conducting Polymer Through a Hydrothermal Polymerization Method and its Application as Energy Storage Electrodes" **Nanoscale Research Letters** 14(1): 226. DOI: [10.1186/s11671-019-3051-6](https://doi.org/10.1186/s11671-019-3051-6).
- [29] J. Peng, Z. Zhao, M. Zheng, B. Su, X. Chen, and X. Chen, (2020) "Electrochemical synthesis of phosphorus and sulfur co-doped graphene quantum dots as efficient electrochemiluminescent immunomarkers for monitoring okadaic acid" **Sensors and Actuators, B: Chemical** 304: 127383. DOI: [10.1016/j.snb.2019.127383](https://doi.org/10.1016/j.snb.2019.127383).
- [30] R. V. Nair, R. T. Thomas, V. Sankar, H. Muhammad, M. Dong, and S. Pillai, (2017) "Rapid, Acid-Free Synthesis of High-Quality Graphene Quantum Dots for Aggregation Induced Sensing of Metal Ions and Bioimaging" **ACS Omega** 2(11): 8051–8061. DOI: [10.1021/acsomega.7b01262](https://doi.org/10.1021/acsomega.7b01262).
- [31] F. Sharif, A. S. Zeraati, P. Ganjeh-Anzabi, N. Yasri, M. Perez-Page, S. M. Holmes, U. Sundararaj, M. Trifkovic, and E. P. Roberts, (2020) "Synthesis of a high-temperature stable electrochemically exfoliated graphene" **Carbon** 157: 681–692. DOI: [10.1016/j.carbon.2019.10.042](https://doi.org/10.1016/j.carbon.2019.10.042).
- [32] H. Huang, S. Yang, Q. Li, Y. Yang, G. Wang, X. You, B. Mao, H. Wang, Y. Ma, P. He, Z. Liu, G. Ding, and X. Xie, (2018) "Electrochemical Cutting in Weak Aqueous Electrolytes: The Strategy for Efficient and Controllable Preparation of Graphene Quantum Dots" **Langmuir** 34(1): 250–258. DOI: [10.1021/acs.langmuir.7b03425](https://doi.org/10.1021/acs.langmuir.7b03425).
- [33] H. Kalita, V. S. Palaparthi, M. S. Baghini, and M. Aslam, (2020) "Electrochemical synthesis of graphene quantum dots from graphene oxide at room temperature and its soil moisture sensing properties" **Carbon** 165: 9–17. DOI: [10.1016/j.carbon.2020.04.021](https://doi.org/10.1016/j.carbon.2020.04.021).
- [34] Z. Zhao, W. Cai, Z. Xu, X. Mu, X. Ren, B. Zou, Z. Gui, and Y. Hu, (2020) "Multi-role p-styrene sulfonate assisted electrochemical preparation of functionalized graphene nanosheets for improving fire safety and mechanical property of polystyrene composites" **Composites Part B: Engineering** 181: 107544. DOI: [10.1016/j.compositesb.2019.107544](https://doi.org/10.1016/j.compositesb.2019.107544).